Effect of internal drainage on performance of reinforced earth wall during rainfall

Yoo, C.
Department of Civil and Environmental Engineering, Sungkyunkwan University, Suwon, Korea

Keywords: reinforced earth wall, rainfall, slope stability, finite element analysis

ABSTRACT: This paper presents the results of a numerical investigation on the effect of internal drainage on the performance of reinforced earth wall during rainfall. A series of limit-equilibrium based slope stability analyses within the framework of unsaturated shear strength, coupled with transient infiltration analyses, was conducted with due consideration of a rainfall scenario during monsoon season in Korea. The results show that the horizontal drainage provided by the hybrid geogrid significantly decreases the degree of reduction in matric suction in the reinforced zone during rainfall. It is also shown that the decrease in the global stability factor of safety is smaller when using the hybrid geogrid than the ordinary geogrid during rainfall due to less decrease in matric suction in the reinforced zone.

1 INTRODUCTION

Reinforced earth walls are now being accepted as alternatives to conventional retaining walls due to a number of advantages in terms of cost and expediency of construction as well as sound performance. This is especially true in Korea since its first appearance in the early 1990's, in private sectors. Despite the sound geotechnical principles adopted in the reinforced earth wall design and construction philosophy, there are many areas that need in-depth studies from the geotechnical engineering point of view.

As for most types of retaining walls, there have been a number of reports on rainfall-related damage of reinforced earth walls, covering a range of minor structural damage to total collapse. These problems are usually related to (i) backfilling with improperly draining fine grained soil and (ii) improper drainage system (Koerner & Soong 2001, Yoo and Jung 2006). The importance of backfill material quality and performance of drainage system for reinforced earth walls has been well illustrated by Yoo & Jung (2006). As the global warming related climate change tends to cause locally concentrated heavy rainfalls, the effect of rainfall on the stability of reinforced earth walls needs special attention from the design and construction point of view. The rainfall related stability issue is even more becoming important because it is common practice to use on-site soil as backfill even if the soil does not meet the criteria set by the current widely accepted design approaches, i.e., NCMA (Collin 1997) and FHWA (Elias & Christopher 1997) design guidelines.

Recently, a geogrid that has in-plane drainage capability has been developed and is available in the market. In this study, the effect of internal horizontal drainage on the performance of reinforced earth wall during was examined. A series of limit-equilibrium based slope stability analyses within the framework of unsaturated shear strength, coupled with transient infiltration analyses, were conducted with due consideration of recent rainfall characteristics in Korea. The geogrid with in-plane drainage capability is referred herein as hybrid geogrid (HG) as opposed to the conventional geogrid (CG).

2 PROBLEM CONSIDERED

2.1 *Wall geometry*

This study considered a geogrid reinforced segmental retaining wall with an exposed wall height of $H = 7.9\ m$. The wall is reinforced with $0.7H$ long geogrid having a design strength of 65 kN/m, installed at vertical spacing of 0.6 m. The wall facing was assumed to be constructed with segmental blocks of 200 mm in height and 300 in depth. Note that two construction scenarios, i.e., one with the hybrid geogrid and the other with the conventional geogrid , were considered;.

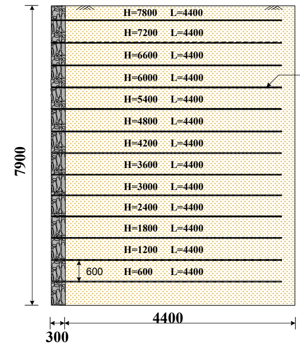

Figure 1. Geometry and reinforcement layout of wall considered.

2.2 *Backfill soil and rainfall characteristics*

In this study, the backfill soil and the rainfall characteristics reported in a reinforced earth wall failure history (Yoo & Jung 2006) were considered. The backfill soil considered is a completely decomposed granite (CDG) soil, classified as SC according to the Unified Soil Classification System (ASTM D2487-90 1992). The soil has effective cohesion and internal friction angle of 13 kPa and 22 deg., respectively, with a saturated permeability of $k_s = 5.0 \times 10^{-7}\ m/s$ and a maximum dry unit weight of $\gamma_{d,\max} = 19\ kN/m^3$. The rainfall considered was June and July rainfalls (Yoo & Jung 2006), each having a precipitation rate of 150 mm/12day and 550 mm/25 day, respectively.

3 TRANSIENT INFILTRATION ANALYSIS

The effect of the in-plane drainage capability of the hybrid geogrid on the pore water pressure development due to the rainfall infiltration was examined using a transient infiltration analysis. The results were then subsequently used in the limit-equilibrium slope stability analyses as will be discussed in a later section.

3.1 *Modeling*

The transient infiltration analysis was conducted using a commercial finite-element program SEEP/W (GeoStudio 2004). In SEEP/W, the saturated and unsaturated flows under steady-state and transient conditions are modeled using the governing equation given in Eq. (1).

$$\frac{\partial}{\partial x}\left(k_w \frac{\partial h_w}{\partial x}\right) + \frac{\partial}{\partial y}\left(k_w \frac{\partial h_w}{\partial y}\right) = m_2^w \rho_w g \frac{\partial h_w}{\partial t} \tag{1}$$

where k_w and h_w represent, respectively, the permeability of soil and the hydraulic head available for flow, m_2^w is the slope of soil water characteristics curve (SWCC) representing the retention characteristics of a soil, ρ_w is the density of water, and g is the acceleration of gravity. An infiltration analysis involving saturated and unsaturated flows also requires a relationship describing hydraulic conductivity at various matric suction values, known as the hydraulic conductivity function (HCF). Figure 2 shows the SWCC and the hydraulic conductivity function for the backfill soil used in the analysis. These curves were inferred from the grain size distribution of a typical backfill soil based on the method proposed by Fredlund et al. (1994).

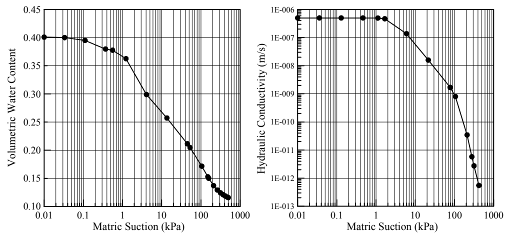

(a) SWCC (b) HCF

Figure 2. SWCC and hydraulic conductivity function for backfill soil.

Figure 3 illustrates the finite-element model adopted for analysis, comprising approximately over 500 four-node plane strain elements. In the model, the wall components, i.e., the wall facing and the hybrid geogrid reinforcement, were explicitly modeled. For the hybrid geogrid in particular, the in-plane horizontal drainage capability was simulated by prescribing a high hydraulic conductivity, $3.3 \times 10^{-5}\ m/s$ given by manufacturer, to 10 mm thick layers of plane strain elements representing the hybrid geogrid. With reference to Figure 3, the initial groundwater table was assumed at 5 m below the bottom of the wall base by prescribing constant head boundaries on the side boundaries, DE and GH. These boundaries were then later allowed to vary in terms of the hydraulic head during the simulation of the rainfall infiltration. No flux was assumed at the bottom boundary EH.

The rainfalls were simulated by prescribing unit fluxes corresponding to the June and July rainfalls on the surface boundaries AF and CB. The wall facing was assumed to have a hydraulic conductivity of $k_s = 5.0 \times 10^{-5}\ m/s$ assuming that the drainage layer behind the wall facing functions well.

After establishing an initial pore water pressure condition in the domain by conducting a steady-state seepage analysis, a transient infiltration analysis simulating the June and July rainfalls was then carried out by applying unit fluxes of 150 mm/12day and 550 mm/25 day, respectively, on the surface boundaries AF and CB. The varying rate of rainfall was simulated by defining a boundary function for the rainfall as a function of time. The adaptive time step feature available in SEEP/W, which allows long time periods to be modeled in a computationally efficient manner, facilitated this procedure.

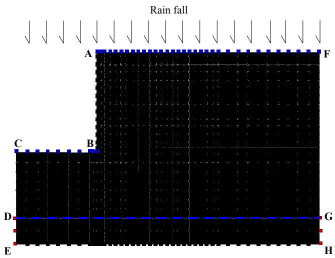

Figure 3. Finite element model adopted

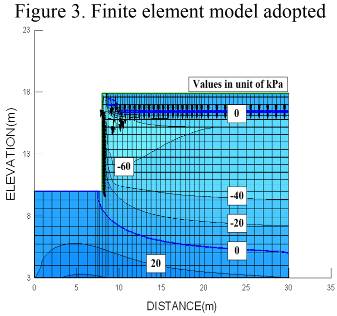

(a) July 1

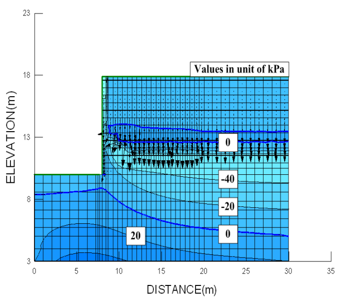

(b) July 30

Figure 4. Pore pressures at different time steps (CR)

3.2 *Pore water pressure distribution*

Figures 4 and 5 show pore water pressure contour plots for the cases analyzed at different elapsed times during rainfall. As seen in Figure 4 for the conventional gegorid, the rainfall in June causes pore water pressure increases in the upper 2 m zone, as much as 60 kPa, resulting in almost no matric suction in that zone. The rainwater infiltration caused by the subsequent July rainfall brings the matric suctions in the reinforced zone further down to almost zero, as illustrated in Figure 4(b), suggesting that the entire reinforced zone, when backfilled with the soil considered in this study, can be fully saturated by the prescribed rainfall. Such a reduction in matric suction caused by the rainfall infiltration in fact decreases the shear strength of the backfill, thereby decreasing the factor of safety of the reinforced wall as will be shown later. For the case with the hybrid geogrid shown in Figure 5, however, it can be seen that the reinforced zone remains unsaturated during the entire rainfall period, showing only approximately 10% reduction in the matric suction.

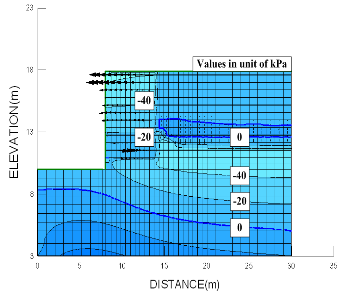

(a) July 1

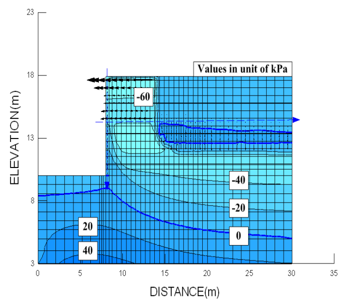

(b) July 30

Figure 5. Pore pressures at different time steps (HR)

The variations of pore pressure with depth at different time steps are illustrated for the two vertical sections of AA' and CC' in Figure 6. As shown, it can be seen for the conventional geogrid case, the pore water pressures are almost zero along depth, while negative pore water pressures prevail for the hybrid geogrid case.

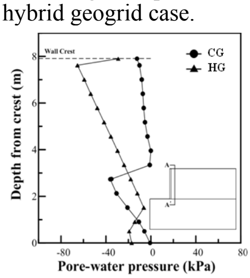

(a) July 1

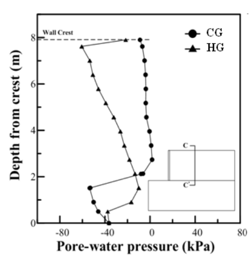

(b) July 30

Figure 6. Comparison of pore water pressure at between CR and HR

4 SLOPE STABILITY ANLAYSIS

A series of limit equilibrium-based slope stability analyses using the SLOPE/W (GeoStudio 2004) was conducted to examine the global stability of the walls during rainfall. In the limit equilibrium-based global slope stability analyses, the pore pressures in the reinforced and retained zones at different rainfall stages from the infiltration analyses were fully considered by taking advantage of the SLOPE/W and SEEP/W interface. SLOPE/W has an ability to incorporate negative pore pressures in the unsaturated zone above the water table in a slope stability analysis, making use of the modified Mohr Coulomb failure criterion [Eq. (2)] proposed by Fredlund et al. (1978) for unsaturated soils to determine the factor of safety:

$$\tau_f = c' + (\sigma - u_a)\tan\phi' + (u_a - u_w)\tan\phi^b \qquad (2)$$

in which τ_f = shear strength, σ =total stress on the failure plane, $(\sigma - u_a)$=net normal stress on the failure plane, and ϕ^b =angle indicating the rate of increase in shear strength relative to the matric suction. Table 1 summarizes the input parameters used in the slope stability analyses. Note that the foundation was assumed to be competent. The factor of safety was obtained using the Bishop's simplified method.

Table 1. Material Properties Used in Slope Stability Analysis

Soil type	c' (kPa)	ϕ' (deg.)	ϕ^b (deg.)	γ (kN/m^3)
Reinforced & retained soils	13	22	10	19
Foundation soil	50	35	20	20

Figure 7 shows the variations of factor of safety (FS) during the rainfalls for different cases. Note that two hybrid geogrid layouts are considered; one in the upper 1/3 zone and the other in the upper 1/2 zone with the remaining zone being reinforced with the conventional geogrid. As shown for the case with the conventional geogrid reinforcement, the initial factor of safety of 2.8 decreases with time to 1.4 at the end of July rainfall due to the decrease in matric suction caused by the rainfall infiltration. For the case with the hybrid geogrid reinforcement cases, however, the factor of safety values remain above 2.0 during the entire rainfall period due to the larger matric suction in the reinforced zone on account of the horizontal drainage capability of the hybrid geogrid. In addition, for the two hybrid geogrid layouts, no significant difference in the factor of safety can be noticed, suggesting that the entire zone needs not be reinforced with the hybrid geogrid. A further study on the optimum layout is required.

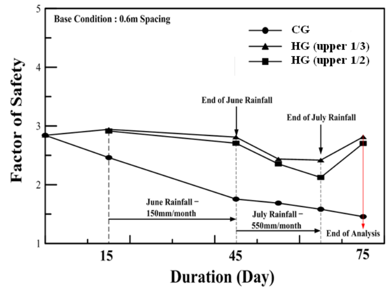

Figure 7. Variations of FS during rainfall

5 CONCLUSIONS

The results of numerical investigation on the effect of internal horizontal drainage on the performance of reinforced earth wall during rainfall are presented. A series of limit-equilibrium based slope stability analyses within the framework of unsaturated shear strength, coupled with transient infiltration analyses, were conducted with due consideration of recent rainfall characteristics in Korea. The results indicate that the internal horizontal drainage help maintain matric suction in the reinforced zone and thus significantly improve stability of the reinforced wall during rainfall.

The results presented in this study demonstrate the potential benefit of a geogrid that also possesses drainage capability for use in reinforced earth wall construction in areas with sever rainfall. A further study on the optimum layout is required.

REFERENCES

Collin, J. 1997. Design Manual for Segmental Retaining Walls, 2nd Ed. National Concrete Masonry Association (NCMA), Virginia, USA.

Elias, V. & Christopher, B.R. 1997. Mechanically Stabilized Earth Walls and Reinforced Soil Slopes, Design and Construction Guidelines. *FHWA Demonstration Project 82*, FHWA, Washington, DC, FHWA-SA-96-071.

Fredlund, D.G.., Morgenstern, N.R. & Widger, A. 1978. Shear strength of unsaturated soils. *Can. Geotech. J.*, Ottawa, 15, pp. 313-321.

Fredlund, D.G., Xing, A., & Juang, S. 1994. Predicting the permeability functions for unsaturated soils using the soil-water characteristic curve. *Can. Geotech. J.*, Ottawa, 31, pp. 533-546.

GeoStudio (2004). "*User's guide for SEEP/W and SLOPE/W*, Version 6.0." Geo-Slope International, Calgary, Canada.

Koerner, R. M. & Soong, T. Y. 2001. Geosynthetic reinforced segmental retaining walls. *Geotextiles and Geomembranes*, 19(6), 359-386.

Yoo, C. & Jung, H.Y. 2006. Case History of Geosynthetic Reinforced Segmental Retaining Wall Failure. *Journal of Geotechnical Engineering* , Vol. 132(12), pp. 1538-1548.